

ON THE NATURE OF VELOCITY FIELDS IN HIGH z GALAXIES

JASON X. PROCHASKA¹, HSIAO-WEN CHEN², ARTHUR M. WOLFE³, MIROSLAVA DESSAUGES-ZAVADSKY⁴, JOSHUA S. BLOOM⁵

Draft version September 10, 2018

ABSTRACT

We analyze the gas kinematics of damped Ly α systems (DLAs) hosting high z gamma-ray bursts (GRBs) and those toward quasars (QSO-DLAs) focusing on three statistics: (1) Δv_{90} , the velocity interval encompassing 90% of the total optical depth, (2,3) W_{1526} and W_{CIV} , the rest equivalent widths of the Si II 1526 and C IV 1548 transitions. The Δv_{90} distributions of the GRB-DLAs and QSO-DLAs are similar, each has median $\Delta v_{90} \approx 80 \text{ km s}^{-1}$ and a significant tail to several hundred km s^{-1} . This suggests comparable galaxy masses for the parent populations of GRB-DLAs and QSO-DLAs and we infer the average dark matter halo mass of GRB galaxies is $\lesssim 10^{12} M_{\odot}$. The unique configuration of GRB-DLA sightlines and the presence (and absence) of fine-structure absorption together give special insight into the nature of high z , protogalactic velocity fields. The data support a scenario where the Δv_{90} statistic reflects dynamics in the interstellar medium (ISM) and W_{1526} traces motions outside the ISM (e.g. halo gas, galactic-scale winds). The W_{1526} statistic and gas metallicity [M/H] are tightly correlated, especially for the QSO-DLAs: $[\text{M/H}] = a + b \log(W_{1526}/1\text{\AA})$ with $a = -0.92 \pm 0.05$ and $b = 1.41 \pm 0.10$. We argue that the W_{1526} statistic primarily tracks dynamical motions in the halos of high z galaxies and interpret this correlation as a mass-metallicity relation with very similar slope to the trend observed in local, low-metallicity galaxies. Finally, the GRB-DLAs exhibit systematically larger W_{1526} values ($> 0.5\text{\AA}$) than the QSO-DLAs ($< W_{1526} > \approx 0.5\text{\AA}$) which may suggest galactic-scale outflows contribute to the largest observed velocity fields.

Subject headings: quasars : absorption lines

1. INTRODUCTION

Absorption-line spectra of quasars have revealed thousands of high redshift galaxies to date (e.g. Wolfe *et al.* 1986; Steidel & Sargent 1992; Prochaska, Herbert-Fort & Wolfe 2005; Prochster, Prochaska & Burles 2006). At $z > 2$, these galaxies are termed the damped Ly α systems (DLAs), absorbers with H I column density $\bar{N}_{\text{HI}} \geq 2 \times 10^{20} \text{ cm}^{-2}$. Although a direct association between star forming galaxies and DLAs is difficult to establish because the background quasar blinds our view (Møller *et al.* 2002), the large N_{HI} values of DLAs indicate large dark matter overdensities (i.e. a virialized system). Furthermore, all of the DLAs show substantial enrichment from heavy metals (Pettini *et al.* 1994; Prochaska *et al.* 2003) and roughly half show indications of ongoing star formation through the presence of C II* absorption (Wolfe, Prochaska & Gawiser 2003). Finally, stars form from neutral gas and the DLAs dominate the atomic hydrogen reservoir at all redshifts (Wolfe *et al.* 1995; Prochaska, Herbert-Fort & Wolfe 2005; Rao, Turnshek & Nestor 2006).

High resolution spectroscopy of DLAs yield precise measurements of the column densities of resonance-line

transitions in the ISM of high z galaxies (Wolfe, Gawiser & Prochaska 2005). Aside from gas-phase abundances, however, it is difficult to derive physical quantities from these observations (e.g. temperature, density). The only other physical characteristic easily studied is the gas kinematics. High-resolution spectra resolve the line profiles of these transitions into ‘clouds’ which trace the velocity fields in young, high z galaxies (Prochaska & Wolfe 1997, 1998). Although it is difficult to reveal the nature of these velocity fields (e.g. rotation, outflows, turbulence) with individual 1-dimensional sightlines, the distributions of kinematic characteristics provide powerful tests for scenarios of galaxy formation (e.g. Jedamzik & Prochaska 1998; Haehnelt, Steinmetz & Rauch 1998).

Prochaska & Wolfe (1997) performed a survey of the kinematic characteristics of neutral gas in DLAs and compared their observations against a variety of simple scenarios. These included rotating disks, clouds with random (virialized) motions, and galactic infall. Observed asymmetries in the observed line-profiles favor rotational dynamics, yet the observed distribution of velocity widths (Δv) has a median too large to be accommodated within standard cold dark matter cosmology. As such, Prochaska & Wolfe (1997) presented these observations as a direct challenge to the basic picture of galaxy formation in a hierarchical universe (e.g. Kauffmann 1996; Mo, Mao & White 1998). In response, theorists introduced additional velocity fields to explain the observations (Haehnelt, Steinmetz & Rauch 1998; McDonald & Miralda-Escudé 1999; Nulsen, Barcons & Fabian 1998; Maller *et al.* 2001). Of particular interest was a model of merging protogalactic clumps where the observed kinematics include contributions from rotation, infall, and random motions (Haehnelt, Steinmetz & Rauch 1998).

¹ Department of Astronomy and Astrophysics, UCO/Lick Observatory; University of California, 1156 High Street, Santa Cruz, CA 95064; xavier@ucolick.org

² Department of Astronomy; University of Chicago; 5640 S. Ellis Ave., Chicago, IL 60637; hchen@oddjob.uchicago.edu

³ Department of Physics, and Center for Astrophysics and Space Sciences, University of California, San Diego, C-0424, La Jolla, CA 92093-0424

⁴ Observatoire de Genève, 51 Ch. des Maillettes, 1290 Sauverny, Switzerland

⁵ Department of Astronomy, 601 Campbell Hall, University of California, Berkeley, CA 94720-3411

While the initial work established this model as a potential solution, recent evaluations using modern numerical simulations and more accurate treatments of radiative transfer have not confirmed its viability (Prochaska & Wolfe 2001; Razoumov *et al.* 2006). The research on kinematic characteristics in DLAs toward quasars (hereafter QSO-DLAs), therefore, tests theories of galaxy formation and gas dynamics in the early universe.

Motivated by these results, we have investigated the dynamics of gas probed by the sightlines to the afterglows of gamma-ray bursts (GRBs). Similar to quasars, the afterglows of GRBs provide bright, albeit transient point-source beacons to the outer universe. With follow-up spectroscopy, one can acquire data at comparable signal-to-noise (S/N) and spectral resolution as quasars (Vreeswijk *et al.* 2004; Fiore *et al.* 2005; Chen *et al.* 2005; Prochaska *et al.* 2007). In turn, one can study the velocity fields of the gas close to the observed beacon. The sightline presumably intersects gas in the star forming region encompassing the GRB, the neutral ISM surrounding it, and gas external to the neutral ISM.

In this paper, we examine the kinematics of a modest sample of damped Ly α systems associated with the ISM surrounding gamma-ray bursts (GRB-DLAs). A principal goal is to characterize the velocity fields of gas observed along these unique sightlines. The data trace velocity fields generated by galactic rotation, gravitational accretion, and any galactic or stellar feedback processes. We will find that these observations reveal new insight for interpretations of the kinematics of gas observed in quasar absorption line studies. Furthermore, we will present a comparison of the GRB-DLA results with those from QSO-DLAs. Comparisons between GRB-DLAs and QSO-DLAs assess the relative galaxy masses and the nature of velocity fields in young, star-forming galaxies.

This paper is organized as follows. Section 2 presents the observational samples and describes the experiment. In § 3, we define statistics for assessing the gas kinematics. § 4 presents the principal results of our analysis and we discuss and interpret these results in § 5.

2. OBSERVATIONAL DATA

We have defined a sample of GRB-DLAs for kinematic analysis based on two primary criteria: (i) the presence of a damped Ly α system ($N_{\text{HI}} \geq 2 \times 10^{20} \text{ cm}^{-2}$) or a low-ion column density that requires N_{HI} exceed $2 \times 10^{20} \text{ cm}^{-2}$ assuming solar metallicity; (ii) spectra with sufficient signal-to-noise and resolution to study the gas kinematics. The latter criterion is not especially strict because we will examine the gas kinematics from equivalent width measurements which do not require high spectral resolution. The sample is also limited to GRB-DLAs where we could access the data or where precise equivalent width measurements are reported in the literature. Figure 1 shows an example set of line-profiles for the GRB-DLA associated with GRB 050820 (Prochaska *et al.* 2007). These data were acquired with the HIRES spectrometer on the Keck telescope and have high spectral resolution ($R \approx 40,000$). The weaker transitions such as Zn II 2026 indicate that the majority (90%) of the gas is localized to one or two ‘clouds’ within a velocity interval of $\approx 50 \text{ km s}^{-1}$. In contrast, the stronger transitions are typically saturated and show absorption spanning nearly 400 km s^{-1} . In the following

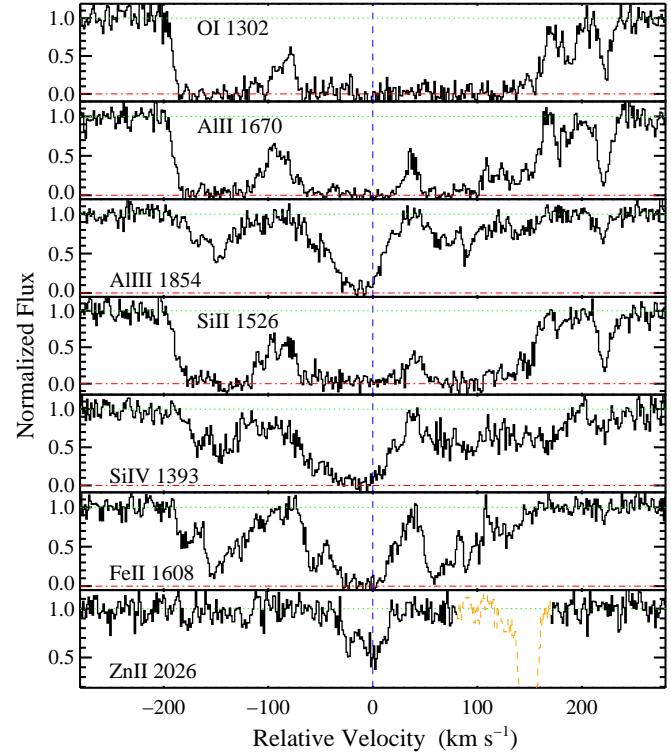


FIG. 1.— Resonance-line profiles for the GRB-DLA associated with GRB 050820 (Prochaska *et al.* 2007). The velocity $v = 0$ corresponds to $z = 2.61469$. Note that the optical depth in low-ion gas is dominated by a few clouds with velocity interval $\Delta v_{90} \approx 50 \text{ km s}^{-1}$ (Zn II 2026). At the same time, there is absorption traced by strong low-ion transitions (e.g. Si II 1526) to velocities of $\approx \pm 200 \text{ km s}^{-1}$.

section, we introduce two kinematic statistics to characterize these properties. Table 1 lists the GRB-DLA comprising our sample, describes the spectral observations, and lists the N_{HI} values and metallicities as described in Prochaska, Chen & Bloom (2007).

Our analysis will frequently draw comparisons between GRB-DLA measurements and QSO-DLA values. For the latter, we will consider two samples of QSO-DLAs, one a subset of the other. The complete sample is drawn from echelle and echelle observations of quasars acquired with the HIRES (Vogt *et al.* 1994) and ESI (Sheinis *et al.* 2000) spectrometers at the Keck Observatory and the UVES (Dekker *et al.* 2000) spectrometer at the VLT Observatory. The data are summarized in these papers: Herbert-Fort *et al.* (2006); Ledoux *et al.* (2006); Dessauges-Zavadsky *et al.* (2006); Prochaska *et al.* (2007). We will restrict the samples to $z_{\text{DLA}} > 1.6$ and DLAs which are greater than 3000 km s^{-1} from their background quasar. The full dataset is a heterogeneous sample of QSO-DLAs including systems selected on the basis of strong metal-lines (Herbert-Fort *et al.* 2006) or targeted for H₂ absorption (Ledoux, Petitjean & Srianand 2003). As such, Prochaska *et al.* (2007) have noted that the H I distribution $f(N_{\text{HI}})$ of this full sample does not follow the statistical distribution⁶ derived from a random survey of background quasars (e.g. Prochaska,

⁶ The QSO-DLAs observed at high spectral resolution have systematically fewer systems with $N_{\text{HI}} \approx 2 \times 10^{20} \text{ cm}^{-2}$, presumably because the observers wished to avoid including absorbers right at the threshold.

TABLE 1
GRB-DLA SAMPLE

GRB	RA	DEC	z_{GRB}	$\log N_{HI}$	f_{mtl}^a	[M/H]	$\sigma([M/H])$	Instrument	R	Ref
GRB990123	15:25:30.34	+44:45:59.1	1.600	22 ^b	12	-0.97		Keck/LRIS	1,000	1
GRB000926	17:04:09.00	+51:47:10.0	2.038	21.30 ^{+0.25} _{-0.25}	2	-0.17	0.29	Keck/ESI	5,000	2
GRB010222	14:52:12.55	+43:01:06.2	1.477	22 ^b	12	-1.30		Keck/ESI	5,000	3
GRB011211	11:15:17.98	-21:56:56.2	2.142	20.40 ^{+0.20} _{-0.20}	11	-1.36		VLT/FORS2	1,000	1,4
GRB020813	19:46:41.87	-19:36:04.8	1.255	22 ^b	12	-1.17		Keck/LRIS	1,000	5
GRB030226	11:33:04.93	+25:53:55.3	1.987	20.50 ^{+0.30} _{-0.30}	11	-1.31		Keck/ESI	5,000	6
GRB030323	11:06:09.40	-21:46:13.2	3.372	21.90 ^{+0.07} _{-0.07}	12	-0.87		VLT/FORS2	1,000	7
GRB050401	16:31:28.82	+02:11:14.8	2.899	22.60 ^{+0.30} _{-0.30}	12	-1.57		VLT/FORS2	1,000	8
GRB050505	09:27:03.20	+30:16:21.5	4.275	22.05 ^{+0.10} _{-0.10}	11	-1.25		Keck/LRIS	1,000	9
GRB050730	14:08:17.14	-03:46:17.8	3.969	22.15 ^{+0.10} _{-0.10}	4	-2.26	0.14	Magellan/MIKE	30,000	10
GRB050820	22:29:38.11	+19:33:37.1	2.615	21.00 ^{+0.10} _{-0.10}	4	-0.63	0.11	Keck/HIRES	30,000	11
GRB050904	00:54:50.79	+14:05:09.4	6.296	21.30 ^{+0.20} _{-0.20}	11	-1.10		Subaru/FOCAS	1,000	12
GRB050922C	19:55:54.48	-08:45:27.5	2.199	21.60 ^{+0.10} _{-0.10}	4	-2.03	0.14	VLT/UVES	30,000	13
GRB051111	00:08:17.14	-00:46:17.8	1.549	22 ^b	12	-0.96		Keck/HIRES	30,000	14,11
GRB060206	13:31:43.42	+35:03:03.6	4.048	20.85 ^{+0.10} _{-0.10}	4	-0.85	0.18	WHT/ISIS	4,000	15
GRB060418	15:45:42.40	-03:38:22.80	1.490	22 ^b	2	-1.65	1.00	Magellan/MIKE	30,000	11

REFERENCES. — 1: Savaglio, Fall & Fiore (2003); 2: Castro *et al.* (2003); 3: Mirabal *et al.* (2002); 4: Vreeswijk *et al.* (2006); 5: Barth *et al.* (2003); 6: Shin *et al.* (2006); 7: Vreeswijk *et al.* (2004); 8: Watson *et al.* (2006); 9: Berger *et al.* (2006); 10: Chen *et al.* (2005); 11: Prochaska *et al.* (2007); 12: Kawai *et al.* (2006); 13: Piranomonte *et al.* (2007); 14: Prochaska, Chen & Bloom (2006); 15: Fynbo *et al.* (2006)

^aFlag describing the metallicity measurement [M/H]: 0=No measurement; 1=Si measurement; 2=Zn measurement; 3=Combination of limits; 4=S measurement; 11=Lower limit from $[\alpha/H]$; 12=Lower limit from Zn

^bBecause $z_{GRB} \leq 1.6$, Ly α was not observed. We have set $N_{HI} = 10^{22} \text{ cm}^{-2}$, the median value of GRB-DLA.

Herbert-Fort & Wolfe 2005). Therefore, we define a pseudo-statistical sample of QSO-DLAs by restricting the list to the QSO-DLAs compiled by Prochaska *et al.* (2003). Although the DLA in this subset also do not follow the $f(N_{HI})$ distribution of a random sample, they were selected only on the basis of a large H I column density, i.e. independent of any kinematic characteristic or chemical abundance.

We have analyzed the kinematic properties from our own HIRES and ESI observations and supplemented these measurements with the results presented in Ledoux *et al.* (2006) from UVES data acquired with the VLT. For equivalent width measurements, however, we have derived values only from our HIRES and ESI observations (Prochaska *et al.* 2007; Herbert-Fort *et al.* 2006). These values have typical statistical uncertainties of less than 0.02Å.

In a previous paper (Prochaska, Chen & Bloom 2007), we discussed why the parent populations of galaxies hosting QSO-DLAs and GRB-DLAs may be different (e.g. gas cross-section selected versus current SFR selected) and how the sightline configurations are fundamentally distinct. The GRB-DLAs do exhibit larger N_{HI} , metallicity, α/Fe , and depletion levels than QSO-DLAs (Prochaska, Chen & Bloom 2007), but we argued that the differences do not require distinct parent populations of galaxies. Instead, the observations imply sightlines with smaller average impact parameter through high z galaxies. This conclusion is expected for a sample selected by gas cross-section (QSO-DLA) versus ones restricted to originate in star-forming regions (GRB-DLA). The cartoon in Figure 2 illustrates these ideas. While QSO-DLAs preferentially penetrate the outer regions of the ISM, the GRB-DLA sightlines originate within their host galaxies, presumably within an H II region generated by its progenitor and other O and B stars. This

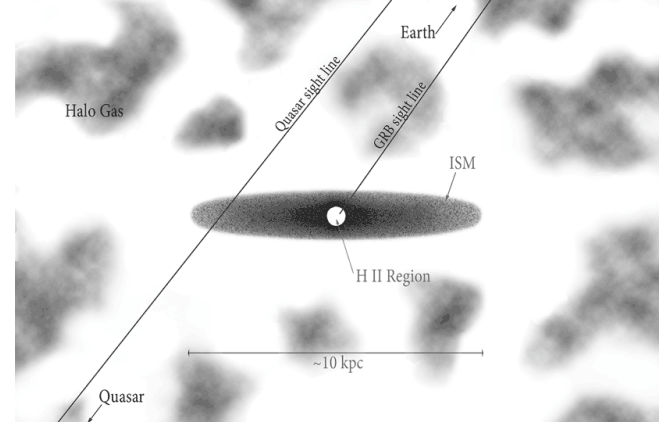


FIG. 2.— This cartoon illustrates the likely differences between QSO-DLA and GRB-DLA sightlines. The former have randomly intersected a foreground galaxy. These QSO-DLA sightlines correspond to a cross-section selected sample and should preferentially intersect the outer regions of the ISM in high z galaxies. In contrast, the GRB-DLA sightlines are constrained to originate from within the ISM of their host galaxies, presumably the H II region produced by massive stars in a star-forming region. These GRB-DLA sightlines are expected (and observed) to originate within the inner few kpc of the ISM.

has two key implications for the gas kinematics: (i) the GRB-DLA observations will probe only a fraction of the velocity field along the full sightline; (ii) each GRB-DLA sightline is biased to intersect its own star forming region. We expect these regions to have very small cross-section to QSO-DLA sightlines (Zwaan & Prochaska 2006) and to be rarely probed by such samples. In this respect, GRB-DLAs may open a new window into the velocity fields of high z galaxies (c.f. Pettini *et al.* 2001).

3. KINEMATIC DIAGNOSTICS

With high resolution observations, one resolves the absorption-line profiles of unsaturated transitions into

TABLE 2
GRB-DLA KINEMATIC CHARACTERISTICS SUMMARY

GRB	λ_{low} (Å)	Δv_{low} (km s $^{-1}$)	W_{1526} (Å)	W_{CIV} (Å)
GRB000926	2026.136	280	2.40 ± 0.14	> 2.20
GRB010222	2056.254	100	1.51 ± 0.13	> 2.55
GRB011211			1.35 ± 0.19	0.70 ± 0.13
GRB020813	2260.780	210	1.71 ± 0.10	1.53 ± 0.05
GRB030226	2374.461	340 ^a	0.97 ± 0.02	0.32 ± 0.02
GRB030323			0.75 ± 0.03	1.50 ± 0.03
GRB050401			2.31 ± 0.26	1.28 ± 0.26
GRB050505			1.81 ± 0.10	> 5.92
GRB050730	1741.553	25	0.37 ± 0.01	0.81 ± 0.01
GRB050820	2026.136	55	1.65 ± 0.01	1.51 ± 0.01
GRB050922C	1608.451	89	0.52 ± 0.01	0.75 ± 0.01
GRB051111	2249.877	31	0.79 ± 0.20	1.35 ± 0.20
GRB060418	2576.877	57	0.66 ± 0.02	0.80 ± 0.02

NOTE. — All EW values reported are rest-frame equivalent widths.

^aEstimated from Figure 2 of Shin *et al.* (2006). Because the line-profiles are partially saturated, this value may be considered an upper limit.

individual components, frequently termed ‘clouds’. The clouds in QSO-DLAs have typical Doppler widths of $b = \sqrt{2}\sigma \approx 5 - 10$ km s $^{-1}$ (e.g. Dessauges-Zavadsky *et al.* 2006). The dispersion results from macroscopic motions (e.g. turbulence) not thermal broadening; the latter imply temperatures that would collisionally ionize the gas. The GRB-DLAs show clouds with similar characteristics that comprise the observed line-profiles (Figure 1; Fiore *et al.* 2005; Chen *et al.* 2005; Prochaska *et al.* 2007).

One can characterize the velocity field along the sightline by tracing the motions of these clouds. Presently, we do not have measurements of the systemic redshifts for our sample of GRB host galaxies (e.g. via nebular lines). Therefore, we will primarily discuss relative velocities. Standard practice is to define a velocity width Δv_{90} as the interval which encompasses 90% of the total optical depth of the gas. This definition was introduced in part to limit a single, weak cloud or statistical fluctuations from dominating the statistic (Prochaska & Wolfe 1997). Following the approach for QSO-DLAs (Prochaska & Wolfe 1997, 1998, 2001; Ledoux *et al.* 2006), we measure the Δv_{90} statistic from a single, unsaturated low-ion transition⁷ which, ideally, has relatively high S/N. For the QSO-DLA we demand S/N $> 15\text{pix}^{-1}$ but have relaxed this requirement for the GRB-DLA because of the generally poorer data quality. To resolve the optical-depth profile, however, it is necessary to restrict the sample to echelle or echellette observations. As an example of the procedure, consider the line-profiles in Figure 1 where we measure $\Delta v_{90} = 55$ km s $^{-1}$ using the Zn II $\lambda 2026$ transition. Table 2 summarizes the measurements for the full GRB-DLA sample.

We also introduce a complimentary diagnostic of gas kinematics: the rest equivalent width $W = W_{\text{obs}}/(1+z)$. This quantity has kinematic significance for optically thick (i.e. saturated) transitions. In these cases, the equivalent width is most sensitive to the differential motions of individual clouds as opposed to their column densities. In contrast to Δv_{90} , the W value represents

⁷ Note that Δv_{90} is insensitive to the specific transition analyzed provided the line is unsaturated and is associated with a low-ion (Prochaska & Wolfe 1997).

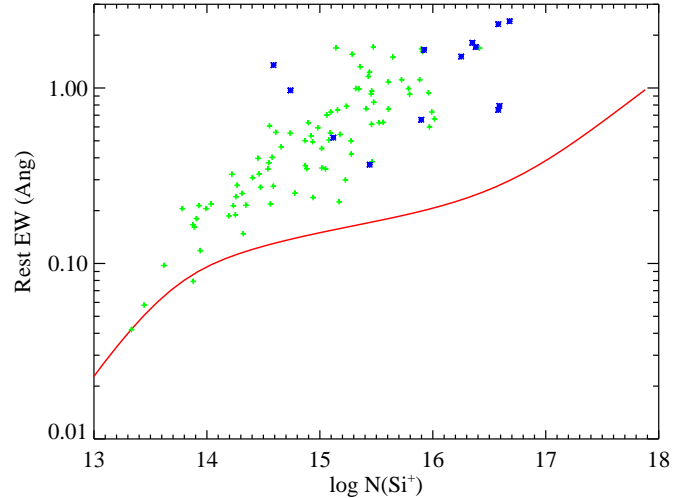


FIG. 3.— Curve-of-growth for the Si II 1526 transition assuming a Doppler parameter $b = 7$ km s $^{-1}$. Overplotted on the figure are the observed total Si $^{+}$ column densities and equivalent widths from the QSO-DLAs (green, plus-signs) and GRB-DLAs (blue stars). Aside from the few QSO-DLAs with very low W_{1526} , the equivalent widths are dominated by the contribution from multiple clouds with a broad range of column densities.

the velocity field of greater than 90% of the gas and can be dominated by clouds with relatively low column density (e.g. Bouché *et al.* 2007). We emphasize that the W value should only be sensitive to the metallicity and/or N_{HI} value of the sightline at very low values, i.e. when the transition is not saturated. Below, we demonstrate that Δv_{90} and W are correlated but with large scatter.

We have measured rest equivalent widths from the Si II $\lambda 1526$ transition (W_{1526}) for low-ion gas and the C IV 1548 transition for high-ion gas. The Si II $\lambda 1526$ transition saturates at $N(\text{Si}^{+}) \approx 10^{14} \text{ cm}^{-2}$ which is 10 \times lower than the Si $^{+}$ column density for any GRB-DLA sightline and 2 \times lower than nearly every QSO-DLA. Therefore, this measure should be relatively insensitive to the gas metallicity or N_{HI} value. This point is emphasized in Figure 3 where we show the curve-of-growth for the Si II 1526 transition and the observed total Si $^{+}$ column density and equivalent widths for the QSO-DLAs and GRB-DLAs. It is evident that the equivalent width has significant contributions from multiple, lower column density clouds. Because C IV is a doublet, the C IV 1548 transition will blend with C IV 1550 when $W_{1548} \gtrsim 2 \text{ \AA}$. In these few cases, we adopt a lower limit for W_{CIV} . The W_{1526} and W_{CIV} values of the GRB-DLA are summarized in Table 2. We also list the metallicity [M/H] measurement (or lower limit) for each GRB-DLA (see Prochaska, Chen & Bloom 2007, for details).

4. RESULTS

In this section, we present the observational results. The next section will discuss the implications.

4.1. Δv_{90} and W_{1526} Distributions

Figure 4a presents the velocity width (Δv_{90}) distributions for the GRB-DLAs and for the statistical subset of QSO-DLAs. The two distributions are similar; the majority of galaxies have $\Delta v_{90} < 100$ km s $^{-1}$ and each sample shows a significant tail out to several hundred km s $^{-1}$. A two-sided Kolmogorov-Smirnov test rules out

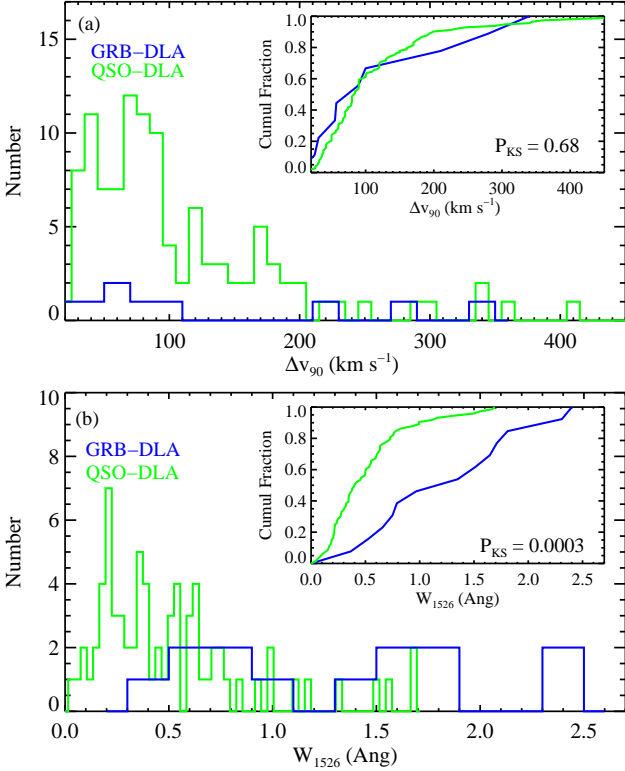


FIG. 4.— Histograms of low-ion kinematic statistics for the GRB-DLAs (dark blue) compared against a statistical sample of QSO-DLAs (light green). The upper panel shows the results for the Δv_{90} statistic, the velocity interval containing 90% of the optical depth of the low-ion gas. The two samples have similar distributions with median $\Delta v_{90} \approx 80 \text{ km s}^{-1}$ and a significant tail to several hundred km s^{-1} . The lower panel shows the equivalent widths of the Si II 1526 transition. In contrast to the Δv_{90} statistic, the GRB-DLAs exhibit systematically larger W_{1526} values than the QSO-DLAs. In both panels, the inset shows the cumulative distributions of the systems, normalized to unity, and the P_{KS} value gives the probability that the two distributions are drawn from the same parent population.

the null hypothesis that the two distributions are drawn from the same parent population at only 32% c.l. In the current GRB-DLA sample, there is a higher fraction of systems with $\Delta v_{90} > 200 \text{ km s}^{-1}$ than the QSO-DLA distribution. The difference is not statistically significant at present, but future observations may reveal a systematic difference in this respect.

Because the GRB are embedded within the interstellar medium (Figure 2), the velocity widths are likely an underestimate of the value that one would derive by extending the sightline through the other side of the galaxy. If the kinematics are dominated by random motions or rotational dynamics, then the median increase in Δv_{90} should be less than a factor of two. To be conservative, we have recomputed the K-S statistic after doubling each Δv_{90} value of the GRB-DLAs. We find results that are still consistent with the null hypothesis, $P_{KS} = 0.08$. In this regard, the sample of GRB-DLA sightlines have velocity fields typical of those observed for QSO-DLAs. Under the assumption that Δv_{90} is dominated by the gravitational potential (e.g. Haehnelt, Steinmetz & Rauch 1998), these results suggest that the parent populations of GRB-DLA and QSO-DLA have similar dynamical masses.

From even the first afterglow spectrum (Metzger *et al.*

1997), it was evident that the gas surrounding GRB exhibit large equivalent widths from low-ion transitions like Si II $\lambda 1526$ and Mg II $\lambda 2796$ (Savaglio, Fall & Fiore 2003). As noted in § 3, these large equivalent widths do not require large N_{HI} or metallicity; the values are often dominated by the velocity fields of low column density clouds which do not contribute to the Δv_{90} statistic. Figure 4b presents a histogram of W_{1526} values for the GRB-DLA compared against the values of the statistical QSO-DLA subset. The mean and median of the GRB-DLA distributions are significantly larger than the QSO-DLAs and a K-S test rules out the null hypothesis at 99.9% c.l. Whereas the Δv_{90} values are in rather good agreement between the two samples, the W_{1526} values of the GRB-DLAs are systematically larger. This is an unexpected and puzzling result which requires unique velocity fields from low column density gas along GRB sightlines.

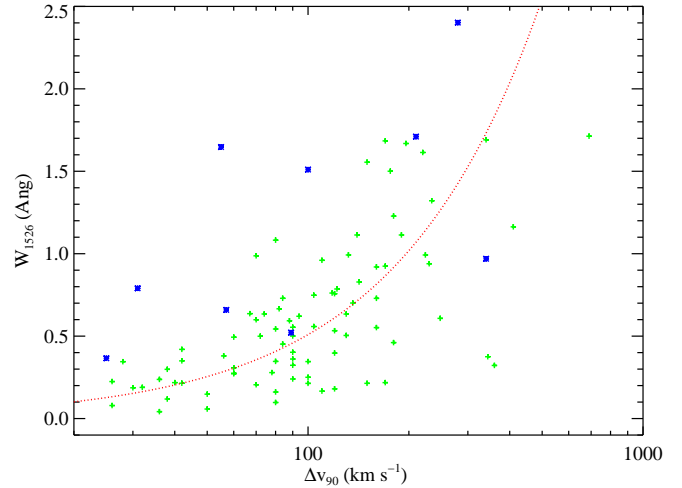


FIG. 5.— Plot of $\Delta v_{90}, W_{1526}$ pairs for the QSO-DLAs (light green) and GRB-DLAs (dark blue) samples. The red dashed-line indicates the W_{1526} value for a boxcar line-profile with velocity width Δv_{90} , i.e. $W_{1526} = \Delta v_{90} * 1526.7066/c$. The sightlines that lie significantly above this curve must have contributions to W_{1526} from gas at large velocity and with less than 10% of the optical depth.

We will argue below that the Δv_{90} statistic in GRB-DLAs is dominated by the ISM of the GRB host galaxy. It is our expectation that this also holds true for QSO-DLAs. We will also argue that the W_{1526} values result from motions independent of the neutral ISM. If other environments contribute to W_{1526} , then one predicts Δv_{90} to be only loosely correlated with W_{1526} . Figure 5, which plots $\Delta v_{90}, W_{1526}$ pairs for the GRB-DLAs and QSO-DLAs, indicates that this is the case. The dashed line traces the predicted W_{1526} value for a fully saturated (i.e. boxcar) line-profile that has velocity width Δv_{90} . Although the QSO-DLAs roughly follow this line, the GRB-DLAs tend to lie significantly above it. Regarding the QSO-DLAs, we interpret the results in Figure 5 as evidence that many sightlines penetrate gas with velocity fields that are distinct from the majority of gas. Furthermore, this fraction appears to increase with Δv_{90} . In the GRB-DLAs, nearly every sightline shows a substantial contribution to W_{1526} from gas that does not dominate the total optical depth. In § 5, we will discuss the origin

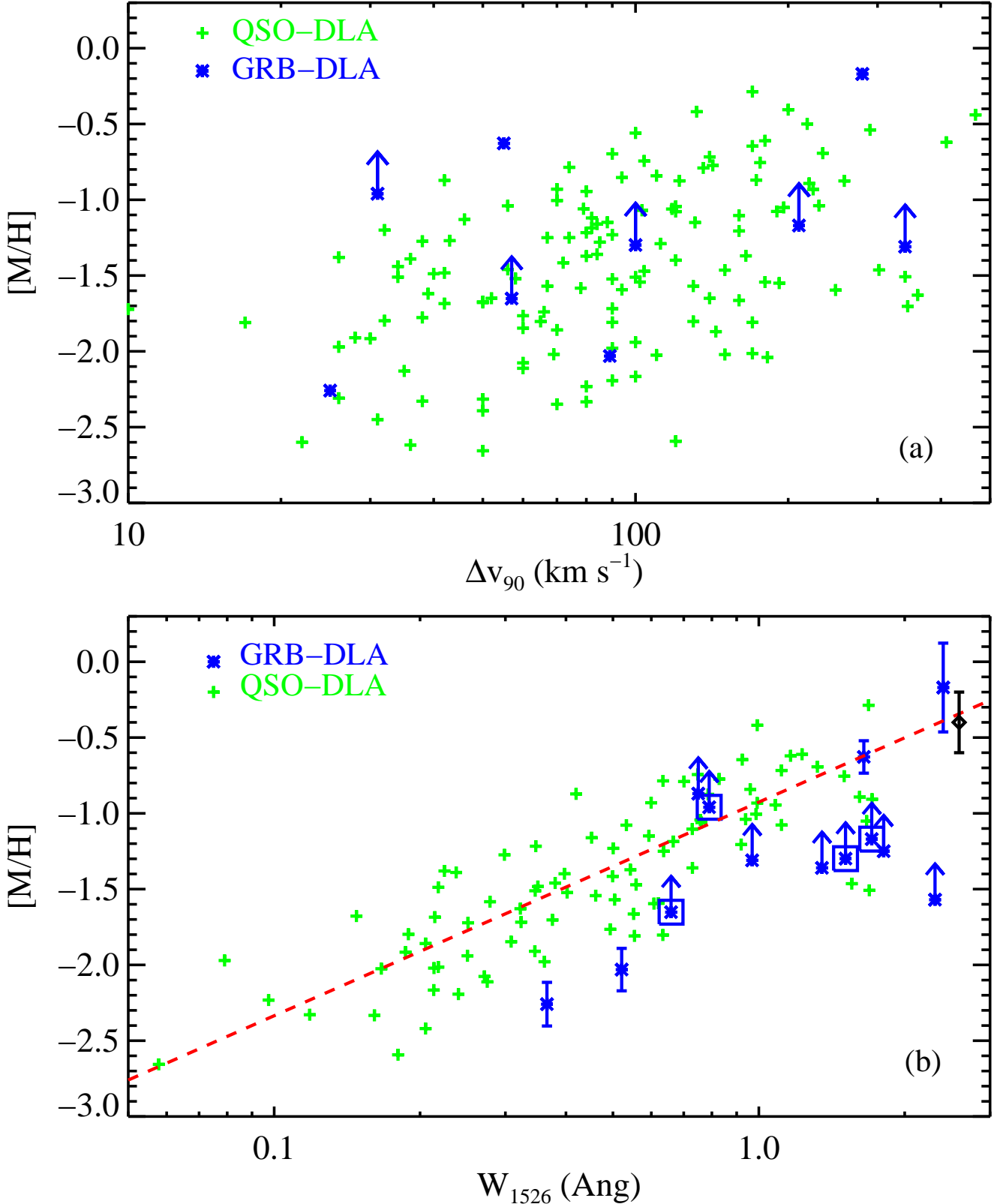


FIG. 6.— Plots indicating correlations between the gas kinematics and metallicity. Upper panel shows pairs of Δv_{90} , $[M/H]$ values for the QSO-DLAs (light green plus-signs) and GRB-DLAs (dark blue stars). The GRB-DLA with lower limits to $[M/H]$ have saturated metal-line profiles while the points marked with squares do not have N_{HI} measurements because they have $z_{\text{abs}} < 1.6$. The QSO-DLAs exhibit a previously discussed correlation (Wolfe & Prochaska 1998; Ledoux *et al.* 2006) and the GRB-DLA appear to trace the same locus. The lower panel compares $[M/H]$ with W_{1526} . The QSO-DLA exhibit a remarkably tight trend, described by the dashed red line: $[M/H] = -0.92 + 1.41 \log(W_{1526}/\text{\AA})$. The GRB-DLAs also appear to show a correlation which may be offset or steeper than the QSO-DLA, but this conclusion is complicated by the preponderance of lower limits. Finally, the black diamond shows the $[M/H], W_{1526}$ values for the Lyman break galaxy CB-58 (Pettini *et al.* 2002). Although its correspondence with the QSO-DLA trend may be coincidence, it is suggestive that large W_{1526} values are related to galactic outflows.

and nature of these velocity fields in greater detail.

4.2. Kinematic Correlations with Other Properties of the ISM

We have considered the trends between kinematic characteristics and other physical properties of the ISM. We first examined whether the GRB-DLAs follow the observed trends for QSO-DLAs between gas kinematics and metallicity (Wolfe & Prochaska 1998; Ledoux *et al.* 2006; Murphy *et al.* 2007). Figure 6a presents $[M/H]$ values against the Δv_{90} statistic for the GRB-DLAs and the full QSO-DLA sample. Note that the GRB-DLA data points with lower limits to $[M/H]$ have $z_{abs} < 1.6$ and an assumed H I column density $N_{HI} = 10^{22} \text{ cm}^{-2}$. Therefore, these $[M/H]$ values (reported as lower limits because their metal-line profiles are saturated) should be considered cautiously. The QSO-DLAs shown in Figure 6a exhibit the correlation reported by previous authors (Wolfe & Prochaska 1998; Ledoux *et al.* 2006). It is not a tight trend, however, and we suspect several physical factors (e.g. a mass/metallicity relation; variations with sightline impact-parameter and galaxy inclination) contribute to produce the observed distribution. Similar to the Δv_{90} distribution (Figure 6a), we find that the GRB-DLAs track the locus defined by the QSO-DLAs. Adopting the upper limits to $[M/H]$ as values, we report a Pearson correlation coefficient of 0.4. We conclude that there is only tentative evidence for a correlation between Δv_{90} and $[M/H]$ for the GRB-DLA.

In Figure 6b, we present the W_{1526} , $[M/H]$ pairs for the two populations. The QSO-DLA data exhibit a remarkably tight correlation. These are well described by a power-law,

$$[M/H] = a + b \log(W/1\text{\AA}) , \quad (1)$$

with best-fit parameters, $a = -0.92 \pm 0.05$ and $b = 1.41 \pm 0.10$. For this fit, we have assumed equal weights for all of the data points and we have restricted the sample to $W_{1526} < 1.4\text{\AA}$ to ignore the ‘outliers’ at large W_{1526} value. If we include all of the data points (with equal weighting), we derive $a = -1.00 \pm 0.05$ and $b = 1.27 \pm 0.10$. Although the data scatter about this power-law, the trend is considerably tighter than the correlation between Δv_{90} and $[M/H]$. In fact, it is the tightest correlation known between metallicity and any other property of the QSO-DLAs (see also Murphy *et al.* 2007). The small scatter is especially impressive given that ≈ 0.15 dex is expected from observational uncertainty in the $[M/H]$ measurements (N_{HI} error). It is a rather surprising trend because the kinematics of the gas that determines $[M/H]$ are better described by the Δv_{90} statistic yet Figure 6a shows this correlation has much greater scatter. Put another way, the line-profiles with $W_{1526} > 0.3\text{\AA}$ are highly saturated and should not be expected to reflect the gas metallicity (Figure 3).

This is not to imply that the W_{1526} values are strictly independent of $[M/H]$. For example, an optical depth profile characterized by shallow, decreasing wings extending to large velocity (e.g. a Lorentzian profile) would yield larger W_{1526} for larger $N(\text{Si}^+)$. On the other hand, a velocity field with a sharp cutoff (e.g. a Gaussian random field) would be insensitive to $[M/H]$. Furthermore, the peak optical depth value is a function of both $[M/H]$ and N_{HI} , and the QSO-DLA data presented in Figure 6b

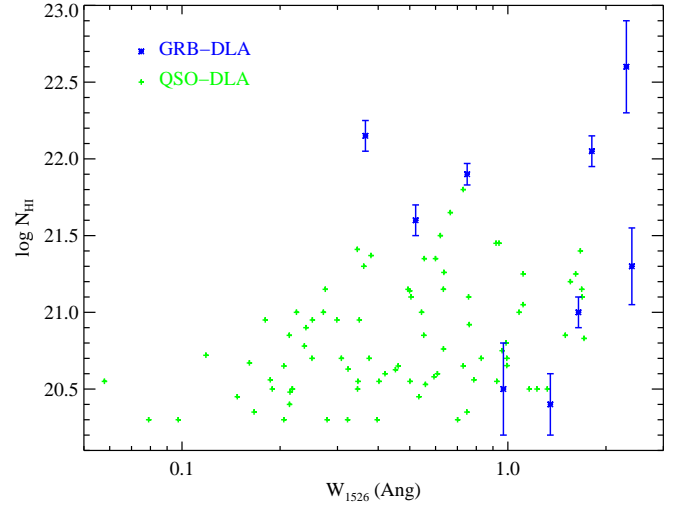


FIG. 7.— Pairs of W_{1526} , N_{HI} values for the QSO-DLAs (light green) and GRB-DLAs (dark blue). Regarding the QSO-DLA, systems with larger W_{1526} show larger N_{HI} value on average, yet the correlation shows large scatter. Similarly, the GRB-DLA sample is characterized by a large scatter but without any obvious trend. Although the N_{HI} value and metallicity $[M/H]$ contribute equally to the Si^+ column density and presumably W_{1526} , the latter is tightly correlated only with metallicity.

span a factor of ≈ 1.5 dex in N_{HI} value. Therefore, the results on the QSO-DLAs in Figure 6b indicate an underlying physical mechanism which causally connects $[M/H]$ and W_{1526} . The GRB-DLAs also show a trend between W_{1526} and $[M/H]$, although its characterization is complicated by the many lower limits to $[M/H]$. A qualitative assessment of the current results suggests either an offset between the trends for the two populations and/or a steeper power-law for the GRB-DLAs. We will return to these issues in § 5.3.

Irrespective of the physical origin of the correlation, the results presented in Figure 6b indicate one may use W_{1526} as a proxy for metallicity, especially if applied to a sample of data points instead of individual systems. We find that a sample of at least 10 QSO-DLA systems gives an average logarithmic metallicity derived from the observed W_{1526} values and Equation 1 that lies within 20% of the actual value for 95% of random trials. Emboldened by this result, we apply equation 1 to the GRB-DLAs but offsetting $[M/H]$ by δ_{MH} to allow for an offset between the GRB-DLA and QSO-DLA trends. We derive an average logarithmic metallicity for the GRB of $< [M/H] > = -0.8 + \delta_{MH}$.

We have also examined trends between W_{1526} and the H I column density (for Δv_{90} vs. N_{HI} , see Wolfe & Prochaska 1998; Wolfe, Gawiser & Prochaska 2005). Figure 7 presents the W_{1526} , N_{HI} pairs for the QSO-DLAs and GRB-DLAs. The two quantities are correlated in that the median N_{HI} value increases with W_{1526} . Furthermore, there are no sightlines with low W_{1526} and large N_{HI} value. For sightlines with $W_{1526} > 0.3\text{\AA}$, however, we observe a wide range of N_{HI} values for any given W_{1526} value. The large observed scatter contrasts with the $[M/H]$, W_{1526} trends in Figure 6b, even though $N(\text{Si}^+)$ is the product of $[M/H]$ and N_{HI} . We conclude that only $[M/H]$ is physically tied to the gas kinematics expressed by the W_{1526} statistic.

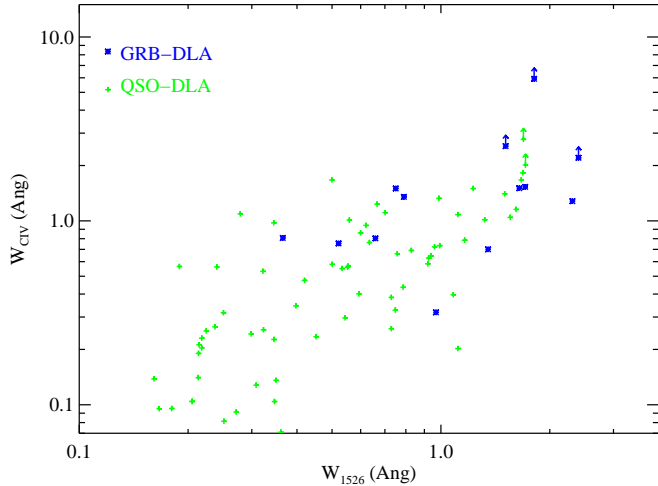


FIG. 8.— Gas kinematics of high-ions (W_{CIV}) compared against low-ion kinematics (W_{1526}) for the QSO-DLA (light green) and GRB-DLA (dark blue) samples. The two quantities are clearly correlated for the QSO-DLAs, whereas the GRB-DLAs exhibit too small of a dynamic range to robustly exhibit any trend.

4.3. High-ion gas: W_{CIV}

It is difficult to measure the 90% velocity interval for C IV in GRB-DLAs because the C IV doublet is often saturated. Therefore, we have examined the rest equivalent width of the C IV 1548 transition, W_{CIV} . These are plotted against W_{1526} in Figure 8. Even though unsaturated low-ion profiles do not closely track the C IV line-profiles in QSO-DLAs (i.e. component by component; Wolfe & Prochaska 2000), there is a strong correlation between their low and high-ion kinematics. Wolfe & Prochaska (2000) have interpreted this global correlation as an indication that the gas traces the same gravitational potential (see also Maller *et al.* 2003).

The GRB-DLAs also exhibit a significant correlation between W_{1526} and W_{CIV} . But, one also finds that the W_{CIV} values of the GRB-DLA are systematically larger than those for the QSO-DLAs. Similarly, W_{CIV} correlates with the ISM metallicity for both samples. The correlation between W_{CIV} and W_{1526} in the GRB-DLAs suggests that their velocity fields are at least coupled. This assertion is further supported by the coincidence of C IV and Si II $\lambda 1526$ absorption at some velocities (Prochaska *et al.* 2007). Therefore, investigations on the velocity field of one ion may give insight to the other.

5. DISCUSSION

5.1. Summary of Results

The results presented in the previous section can be summarized as follows:

1. The distributions of Δv_{90} values (the velocity interval encompassing 90% of the gas) from QSO-DLAs and GRB-DLAs are very similar. Both samples exhibit median $\Delta v_{90} \approx 80 \text{ km s}^{-1}$ with a significant tail to several hundred km s^{-1} (Figure 4a).
2. In contrast to the Δv_{90} statistic, the GRB-DLA exhibit systematically larger W_{1526} measurements than the QSO-DLAs (Figure 4b).
3. Both the GRB-DLAs and QSO-DLAs show a correlation between Δv_{90} and metallicity [M/H] but

with large scatter (Figure 6a).

4. There is a remarkably tight correlation between W_{1526} and metallicity [M/H] for the QSO-DLA sample. The correlation is well described by a power-law, $[\text{M/H}] = a + b \log(W_{1526}/1\text{\AA})$ with $a = -0.92 \pm 0.05$ and $b = 1.41 \pm 0.10$. There is also a correlation observed between metallicity and W_{1526} for the GRB-DLAs. This trend may be offset and/or steeper than the QSO-DLA distribution (Figure 6b).
5. The high-ion and low-ion kinematics traced by W_{1526} and W_{CIV} are correlated (Figure 8).

We will now explore the origin and nature of the velocity fields in QSO-DLAs and GRB-DLAs and the implications for the galaxies which produce them.

5.2. The Nature of Galactic Velocity Fields at High z

In a star-forming galaxy, there are four principal areas that have unique velocity field characteristics and can contribute to the Δv_{90} and W_{1526} statistics: (i) the neutral ISM, whose motions are dominated by galactic rotation and mild turbulent velocities; (ii) H II regions, with velocity fields driven by stellar processes (e.g. winds, supernovae); (iii) halo gas clouds, whose kinematics include contributions from gravitational accretion and virialized motions; and (iv) galactic-scale outflows driven by supernovae activity in the ISM (e.g. Mac Low & Ferrara 1999) and/or heating by galaxy-galaxy mergers (e.g. Cox *et al.* 2006). In the following, we will examine our observational results within the framework of a model where the Δv_{90} statistic is dominated by gas in the ambient, neutral ISM while halo dynamics determine the the W_{1526} and W_{CIV} measurements. In addition, we will propose that the W_{1526} and W_{CIV} statistics occasionally trace velocity fields representative of galactic-scale outflows.

This two component scenario (ISM+halo gas) is neither an original nor provocative interpretation of absorption-line systems arising in galaxies (e.g. Mo & Miralda-Escude 1996; Kauffmann 1996; Haehnelt, Steinmetz & Rauch 1998; McDonald & Miralda-Escudé 1999; Maller *et al.* 2001, 2003). Indeed, this is also the favored model for gas in the Milky Way (e.g. Spitzer 1990; Savage, Sembach & Lu 1997) and Magellanic Clouds (e.g. Lehner & Howk 2007). And, the model has been invoked for a wide range of quasar absorption-line observations including the impact parameter distribution of Mg II systems from their host galaxies (Bergeron & Boisse 1991; Lanzetta & Bowen 1990, 1992; Steidel 1993) and C IV absorption by galaxies (Chen, Lanzetta & Webb 2001; Wolfe & Prochaska 2000; Maller *et al.* 2003). We will demonstrate that our observations support this model and we will derive new insights into the gas dynamics of high z galaxies.

Within this disk/halo scenario, the Δv_{90} statistic traces the kinematics of the ambient ISM, i.e., the optical depth of the gas external to the neutral ISM contributes less than 10% of the total. In the context of QSO-DLAs, this is reasonable because (i) the large N_{HI} values that define a DLA may require the sightlines intersect the ambient ISM; and (ii) one expects halo gas to be predominantly ionized (e.g. Mo & Miralda-Escude 1996) whereas

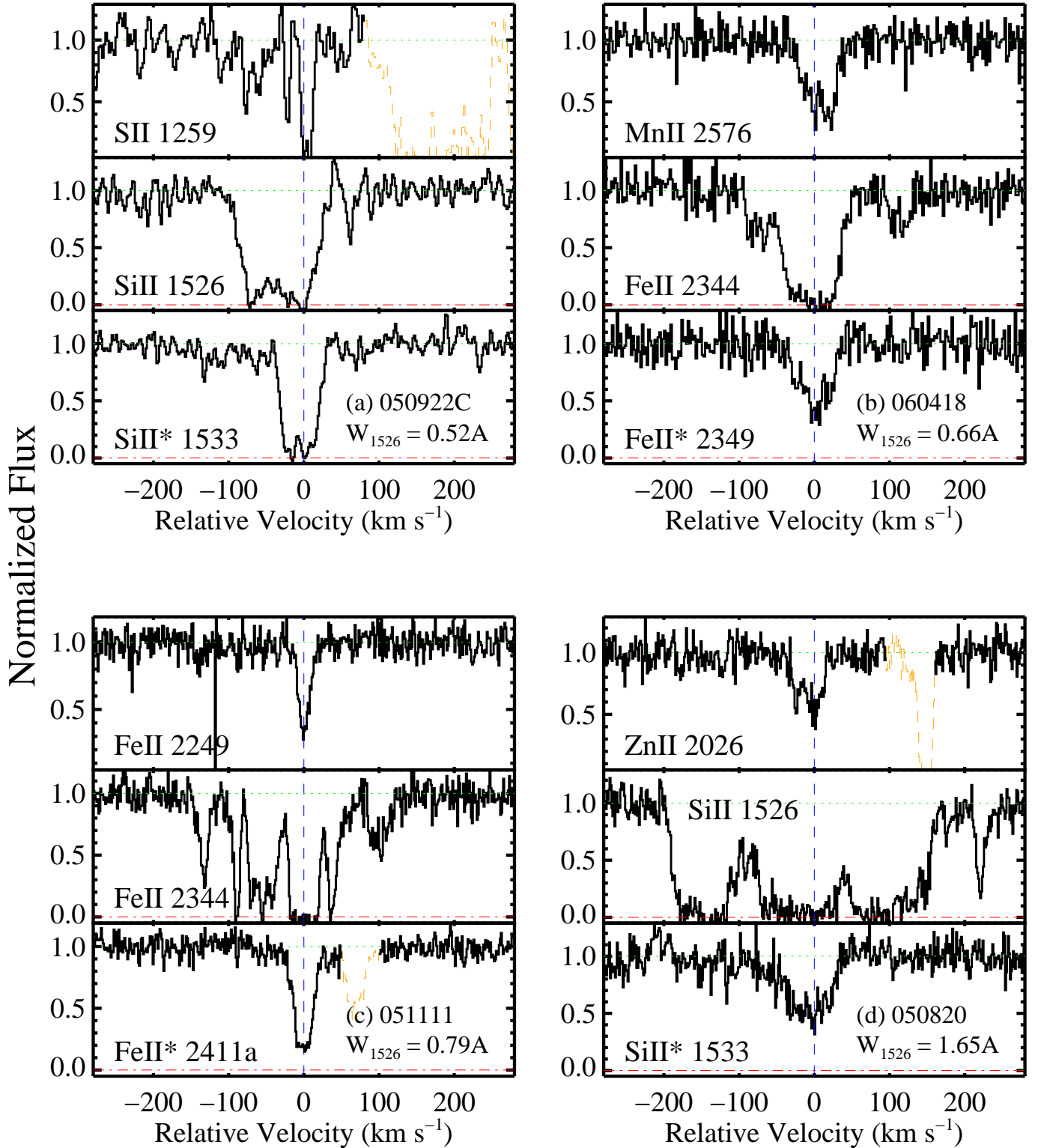


FIG. 9.— These panels show one weak line (top), one strong line (middle) and one fine-structure transition (bottom) for four GRB-DLAs observed at high spectral resolution: (a) GRB-DLA/050922C; (b) GRB-DLA/060418; (c) GRB-DLA/051111; and (d) GRB-DLA/050820. In all four GRB-DLAs, the fine-structure optical depth profile closely matches that of the weak transition. Because this gas must lie within ≈ 1 kpc of the GRB afterglow, these observations indicate the Δv_{90} statistic is determined by the velocity field of the ISM surrounding the GRB. In contrast, there are clouds in the wings of the strong transitions which do not show significant fine-structure absorption and must therefore lie at distance $\gtrsim 1$ kpc from the GRB afterglow. Because the fine-structure absorption defines the systemic velocity of the ISM, the unique geometry of the GRB-DLA sightlines allows one to investigate gas with velocities indicate of outflow (negative) or infall (positive). This experiment offers an unprecedented view into the nature of gas kinematics in high z galaxies.

the majority of gas in QSO-DLA is neutral (Vladilo *et al.* 2001; Prochaska *et al.* 2002). We will now demonstrate that observations of the GRB-DLAs directly connect the neutral ISM with the Δv_{90} statistic.

Figure 9 plots pairs of strong resonance-line transitions (one weak, one strong) against a fine-structure transition for four GRB-DLAs observed at high spectral resolution. In all four cases, the fine-structure absorption lines trace only the gas which dominates the total optical depth, i.e. the gas revealed by the weak transitions. Prochaska, Chen & Bloom (2006) showed that fine-structure absorption in the GRB-DLAs is due to UV pumping by radiation from the GRB event and its afterglow. For the GRB-DLAs shown here, the presence of fine-structure absorption dictates that this gas is located within ≈ 1 kpc of the burst. Furthermore, the GRB-DLAs also show Mg I absorption coincident with the fine-structure lines (Prochaska *et al.* 2007). This requires the gas to lie at $\gtrsim 100$ pc to avoid being photoionized by the GRB afterglow (Prochaska, Chen & Bloom 2006, 2007). The overall implication is that gas comprising 90% of the total optical depth lies between ≈ 100 pc and ≈ 1 kpc from the GRB, i.e. within the nearby ISM⁸. In summation, the GRB-DLA observations give empirical confirmation that the Δv_{90} values reflect the kinematics of the neutral ISM.

Having established a direct association between the Δv_{90} values and the ISM, it is reasonable to assume that these values trace the rotational dynamics and turbulent fields within high z galaxies. This is especially the case for systems with $\Delta v_{90} < 200$ km s $^{-1}$; larger Δv_{90} values may be better interpreted as sightlines through multiple galaxies or even supernovae winds (Nulsen, Barcons & Fabian 1998). Because the turbulent velocities in neutral gas are generally small ($\sigma_{turb} \approx 10$ km s $^{-1}$), sightlines with $\Delta v_{90} > 20$ km s $^{-1}$ should be dominated by differential rotation along the sightline or peculiar motions of multiple massive clumps (Haehnelt, Steinmetz & Rauch 1998; Maller *et al.* 2001). It is natural, therefore, to compare the Δv_{90} distributions of GRB-DLAs and QSO-DLAs in terms of dynamical masses. Before drawing such conclusions using the Δv_{90} distributions, however, one must examine the effects of differences in sightline configuration (Figure 2).

The GRB-DLA sightlines are restricted to travel through approximately half of the galaxy and are expected to have smaller impact parameter than the average QSO-DLA sightline. The latter point is supported by the higher H I column densities, metallicities, and depletion levels observed for GRB-DLA sightlines (Prochaska, Chen & Bloom 2007). These two effects will compete against each other if differential rotation explains the Δv_{90} statistic. On the one hand, a reduced sightline leads to an underestimate of Δv_{90} because one does not probe all of the gas along the sightline. This effect should be small, however, because even a full sightline will only probe approximately one quadrant of a rotating disk (Prochaska & Wolfe 1997). The correction would be larger for a random velocity field, but still less than a factor of two. It is only if the velocity fields are dominated

by a symmetric infall/outflow that the effect would be large. Such velocity fields, however, are unlikely to describe the neutral ISM of high z galaxies. The other geometric effect – smaller average impact parameter – will imply larger Δv_{90} values (e.g. Prochaska & Wolfe 1997). This effect is likely to dominate and, if anything, we expect the GRB-DLAs would be biased to higher Δv_{90} values than the QSO-DLAs for sightlines penetrating the same parent population of galaxies.

We conclude, therefore, that the observed Δv_{90} distributions indicate the galaxies hosting QSO-DLAs and GRB-DLAs have similar mass distributions. There is at least circumstantial evidence in support of this conclusion. In particular, the median luminosity of GRB-DLAs host galaxies is low, approximately $L_*/5$ at $z \sim 1$ (Le Floc'h *et al.* 2003). Although very few QSO-DLA have been successfully imaged at $z > 2$ (Møller *et al.* 2002), theoretical expectation is that the majority will also be sub-luminous (Haehnelt, Steinmetz & Rauch 2000; Maller *et al.* 2000; Nagamine *et al.* 2005) and the average luminosity at $z < 1$ is $L \sim L_*/2$ (Chen & Lanzetta 2003). Similarly, neither sample has shown evidence for a large fraction of bright galaxies (Le Floc'h *et al.* 2003; Colbert & Malkan 2002). Altogether, we conclude that the host galaxies of GRB-DLAs and QSO-DLAs have comparable masses. Adopting recent results on the latter population, we infer dark matter halo masses of $\lesssim 10^{12} M_\odot$ for the GRB-DLA (Bouché *et al.* 2005; Cooke *et al.* 2006; Nagamine *et al.* 2005).

The assertion that GRB-DLA and QSO-DLA host galaxies have similar mass is immediately challenged by our observation that GRB-DLA show systematically larger W_{1526} values (Figure 4b). To address this issue, we must identify the origin of the velocity fields contributing to W_{1526} . There are two factors which contribute to the W_{1526} statistic: the number of clouds intersected by the sightline and the relative velocities of these clouds. The total velocity field is a convolution of the relative velocity field within each environment giving rise to Si $^{+}$ and the relative velocities between the environments. We emphasize that even highly ionized gas can have trace quantities of Si $^{+}$ that would be revealed by the strong Si II $\lambda 1526$ transition (e.g. Prochaska 1999).

Returning to Figure 9, we can address the contribution of various velocity fields to W_{1526} . At small W_{1526} values (a,b), the neutral ISM clearly dominates. In contrast, the two GRB-DLAs with large W_{1526} (c,d) show multiple clouds with relatively low column density and no associated fine-structure absorption. The absence of fine-structure absorption places these clouds at $\gtrsim 1$ kpc from the GRB afterglow (Prochaska, Chen & Bloom 2006; Chen *et al.* 2007). Note that this is true even though the column densities of these components are small compared to the total because the resonance and fine-structure transitions have similar oscillator strengths. Therefore, this gas cannot be associated with star-formation processes local to the GRB (e.g. stellar winds, supernovae). The gas is either within the ISM but at much larger distance than the gas that dominates the total optical depth, or it lies outside the ISM altogether (i.e. halo gas or the ISM of a companion galaxy). We prefer to associate the gas with the galactic halo because: (i) the velocities are large (up to hundreds km s $^{-1}$) compared to random and dynamical motions for the neutral ISM of galaxies; (ii)

⁸ The absence of H₂ absorption in this gas (Tumlinson *et al.* 2007) also indicates we are probing the ambient ISM and not the local star forming region (i.e. molecular cloud).

if the W_{1526} statistic tracked dynamics in the ISM then a very large metallicity gradient may be required for the Δv_{90} statistic to be insensitive to these motions; (iii) there is high-ion absorption (e.g. Si IV, C IV; Figure 1) coincident with many of the low column density Si⁺ components; and (iv) the ionic ratios of some components indicate they are highly ionized (Dessauges-Zavadsky *et al.* 2006). An example of the last point is revealed in Figure 1 by the cloud at $v \approx +200 \text{ km s}^{-1}$. This cloud has $\log[N(\text{O}^0)/N(\text{Si}^+)] = +0.50 \pm 0.05$ even though O is at least 1 dex more abundant than Si in every astrophysical environment known. The only viable explanation for observing $\text{O}^0/\text{Si}^+ \ll (\text{O/Si})_\odot$ is that the gas is highly ionized.

Granted that gas beyond the ISM dominates the W_{1526} statistic, the next issue is to examine the nature of its velocity field. This may include virialized motions, gravitational accretion (Mo & Miralda-Escude 1996; McDonald & Miralda-Escudé 1999), and outflows from galactic feedback (Dong, Lin & Murray 2003; Cox *et al.* 2006). The latter two processes imply organized flows that would be revealed by the observations if we knew the systemic velocity of the galaxy. For the GRB-DLAs, we can measure the systemic redshift from nebular emission lines (e.g. Thoene *et al.* 2006) but the absorption-line data also yield a direct measurement: the line centroid of the fine-structure transitions. Because this gas occurs within $\approx 1 \text{ kpc}$ for the GRB-DLA, it establishes the velocity of the neutral ISM. Examining the line-profiles of Figure 9 (c,d) in this light, we note that the Si⁺ gas shows both positive and negative absorption in the case of GRB-DLA 050820 but predominantly negative velocities for GRB-DLA 051111. Therefore, one example exhibits motions reflective of a random (i.e. virialized) velocity field and the other inspires an outflow interpretation (see also Thoene *et al.* 2006). It is too early to draw generic conclusions about the velocity fields of GRB-DLAs, but future observations akin to Figure 9 will offer an unprecedented view into the nature of gas kinematics at high z .

Let us now address the offset in the W_{1526} distributions between the GRB-DLAs and QSO-DLAs (Figure 4b). Could the offset be explained by differences in sightline configurations? As with the Δv_{90} values, there are competing effects. The bias to smaller impact parameter will only be important if the Si⁺ velocity fields have significant variations on kpc scales. This could occur if the majority of gas is located near star-forming regions, i.e. the origin of the GRB sightline. If the Si⁺ gas is distributed throughout the halo (i.e. tens of kpc), then an impact parameter bias should be unimportant. Meanwhile, if the velocity field has significant contribution from infall or outflow then restricting the GRB-DLA sightlines to originate from within the ISM leads to a systematic underestimate. Therefore, sightline geometry will bias the W_{1526} statistic to larger values for the GRB-DLA only if the velocity field has significant variations on kpc scales and is asymmetric. Numerical simulations do indicate gas being accreted tends to fall in along radial orbits (A. Dekel, priv. comm.). This may imply larger W_{1526} values for sightlines originating at the center of the galaxy (GRB-DLAs) as opposed to large impact parameter (QSO-DLAs). While differences in sightline configurations may contribute to the differences in W_{1526} between QSO-DLAs and GRB-DLAs, we contend that the

observed differences in the W_{1526} distributions for GRB-DLAs and QSO-DLAs reflect actual differences in the gas kinematics of their host galaxies.

A possible explanation for larger W_{1526} values in GRB-DLA is that their host galaxies are significantly more massive. There are two arguments against this assertion. First, the Δv_{90} distributions of the QSO-DLAs and GRB-DLAs are similar (Figure 4a). While the W_{1526} statistic may be a better tracer of the gravitational potential (see below), the Δv_{90} statistic should also distinguish between large differences in dark matter halo masses. Second, direct imaging of GRB host galaxies reveal they have low luminosity (Le Floc'h *et al.* 2003; Fruchter *et al.* 2006) and, presumably, low mass. We consider it unlikely that the QSO-DLA have substantially lower luminosity (and mass) than that observed for the GRB-DLAs.

The most likely interpretation for the higher W_{1526} values in GRB-DLAs is that the kinematics of gas contributing to the W_{1526} statistic has significant contribution from galactic-scale outflows. We are guided to this conclusion in part because the GRB phenomenon is directly linked to active star formation, i.e., GRB host galaxies have systematically higher current star formation rates than QSO-DLA galaxies. One observes that GRB host galaxies have star formation rates which are large for their luminosity (Christensen, Hjorth & Gorosabel 2004). This characteristic is described as a high specific SFR and it separates GRB host galaxies from the general population of high z galaxies. Therefore, a scenario where processes related to star formation stir the velocity fields traced by Si⁺ gas may naturally account for the systematic offset in W_{1526} between QSO-DLAs and GRB-DLAs. These processes may include galactic outflows inspired by major mergers (Cox *et al.* 2006) or galactic fountains driven by supernovae feedback (Mac Low & Ferrara 1999; Dong, Lin & Murray 2003). The latter effect may be challenged, however, by the short lifetime expected for GRB progenitors. In this respect, the velocity fields of GRB-DLAs may more resemble the outflows of the Lyman break galaxies (e.g. Pettini *et al.* 2002). We eagerly await new observations like those presented in Figure 9 to further test these scenarios.

5.3. Interpreting the Kinematic-Metallicity Correlations in DLAs

In Section 4.2 (Figure 6), we presented the observed correlations between the kinematic statistics (Δv_{90} , W_{1526}) and the ISM metallicity [M/H]. The Δv_{90} -[M/H] correlation has been previously identified for QSO-DLA samples (Wolfe & Prochaska 1998; Ledoux *et al.* 2006). Although its scatter is substantial, the statistical significance is high and Ledoux *et al.* (2006) report a best-fit power-law of the form $[\text{M/H}] \propto 1.5 \log \Delta v_{90}$. These authors have interpreted the result in terms of a mass-metallicity relation, i.e. the Δv_{90} statistic traces the gravitational potential of the DLA galaxy. Our results on the GRB-DLA lend further support to this interpretation. In particular, we have shown that the Δv_{90} statistic is dominated by material near the GRB, i.e. the neutral ISM. Although ISM velocity fields are stirred by supernovae, they are generally dominated by gravitational motions (e.g. rotation, turbulence, accretion).

A key aspect of the Δv_{90} -[M/H] trend is its large scat-

ter which cannot be attributed to observational uncertainty. We interpret the scatter as a natural consequence of the QAL experiment. If the velocity field is dominated by rotation, then a large scatter results simply from a range of impact parameters and disk inclinations (e.g. Prochaska & Wolfe 1997). In this case, only the upper bound of the $\Delta v_{90}, [\text{M}/\text{H}]$ locus would describe the average rotation speed of galaxies at a given metallicity. Similarly, if the velocity field results from turbulence or accretion, then Δv_{90} will be sensitive to the number of clouds intersected by the sightline. In this scenario, however, one would require large variations in the number of ‘clouds’ intersected by sightlines, which is not entirely supported by the observations (e.g. Prochaska & Wolfe 1997).

In contrast to the $\Delta v_{90}, [\text{M}/\text{H}]$ trend, the $W_{1526}, [\text{M}/\text{H}]$ pairs for the QSO-DLAs follow an extremely tight correlation (Figure 6b). In fact, most of the scatter may be attributed to observational uncertainty. In several respects, this is a stunning result. The $[\text{M}/\text{H}]$ values represent the average metallicity along the entire sightline, which is dominated, of course, by the gas corresponding to the majority of the total optical depth, i.e., the gas which defines the Δv_{90} statistic. In contrast, gas which has negligible contribution to the measured metallicity can dominate the W_{1526} statistic (Figure 9). Furthermore, we have shown (for the GRB-DLAs) that $[\text{M}/\text{H}]$ is set by gas local to the ISM of the galaxy whereas the W_{1526} statistic has significant contribution from gas external to the ISM. Indeed, quasar absorption lines are frequently associated with halo gas surrounding a galaxy (e.g. Bergeron & Boisse 1991; Steidel 1993; Chen, Lanzetta & Webb 2001; Charlton & Churchill 1998). Therefore, in the DLAs we reach a rather surprising conclusion that the local ISM properties (metallicity) are tightly correlated with the large-scale velocity field.

Let us now comment on the origin of the $W_{1526}, [\text{M}/\text{H}]$ trend. The first point to stress is that we derive a similar power-law as observed for the $\Delta v_{90}, [\text{M}/\text{H}]$ pairs in QSO-DLAs (see also Murphy *et al.* 2007). We conclude that the kinematic-metallicity trends have the same physical origin. One may gain insight by comparing our trend with the velocity-metallicity correlations observed for other galactic populations. Dekel & Woo (2003) have found the velocity dispersion V in dwarf and low-luminosity low surface-brightness galaxies at $z = 0$ correlates with the stellar mass M_* : $V \propto M_*^{0.24}$. Furthermore, their compilation shows a tight correlation between metallicity and stellar mass, $\text{M}/\text{H} \propto M_*^{0.40}$ implying a metallicity-velocity correlation: $\text{M}/\text{H} \propto V^{1.66}$. The correspondence between the kinematic-metallicity trend of local low-mass galaxies with that of the QSO-DLAs is remarkable. Although one refers to this trend locally as a mass-metallicity relation, it is important to stress that simple scaling laws do not predict the observed trend. Dekel & Woo (2003) have shown that in a closed-box model the metallicity is independent of stellar mass; indeed, this follows observations for massive, high surface brightness galaxies (e.g. Tremonti *et al.* 2004). Therefore, Dekel & Woo (2003) argued that the mass-metallicity trend observed for lower mass galaxies requires supernovae feedback (but see also Lee *et al.* 2006; Tassis, Kravtsov & Gnedin 2006). In this respect, therefore, one may speculate whether the velocity fields

observed in the QSO-DLAs represent gravitational dynamics or feedback processes. Let us now consider arguments for and against each interpretation.

There are several arguments supporting the interpretation of Figure 6 in terms of a mass-metallicity correlation, i.e. that the velocity fields trace the gravitational potential. First, the observed slopes of the Δv_{90} and $W_{1526}, [\text{M}/\text{H}]$ trends follow the same trends as local dwarf and low-luminosity low-surface brightness galaxies (Dekel & Woo 2003) whose velocity dispersions presumably reflect their gravitational potentials. Second, the large scatter in the $\Delta v_{90}, [\text{M}/\text{H}]$ trend can be explained by variations in impact parameter and inclination through the DLA galaxies. Third, a tight trend is reasonable for $W_{1526}, [\text{M}/\text{H}]$ pairs if the W_{1526} statistic is dominated by halo dynamics. For virialized motions characterized by a velocity dispersion σ_{virial} , $W_{1526} \propto n_{\text{cl}}^{1/2} \sigma_{\text{virial}}$ and the scatter in this quantity will be small for a given velocity dispersion σ_{virial} if the number of clouds penetrated by the sightline $n_{\text{cl}} \gg 1$. The latter point is supported by the observations (e.g. Figure 1). Fourth, the Si II 1526 profiles of at least some GRB-DLAs show both negative and positive velocities relative to the systemic (Figure 9). This is expected for gas that traces a virialized (random) velocity field (see also Robertson & Chen, in prep.). Finally, Möller, Fynbo & Fall (2004) have noted that the only DLAs that have been successfully imaged at $z \gtrsim 2$ also have high metallicity, suggesting stellar mass may correlate with enrichment.

There are two counterarguments to interpreting the Δv_{90} and W_{1526} statistics as tracers of the gravitational potential of individual dark matter halos. First, it is may be unrealistic to explain velocity widths that exceed several hundred km s^{-1} in terms of a single galactic potential. At very large Δv_{90} or W_{1526} values, therefore, we expect that additional velocity fields contribute. These could include galactic-scale outflows but also the peculiar motions of multiple galaxies along the sightline (e.g. Maller *et al.* 2001). Second, Bouché *et al.* (2007) have reported an anti-correlation between Mg II equivalent width⁹ and the cluster-length of these absorbers (a subset include DLAs Prochster *et al.* 2006) with large, red galaxies (LRGs). These authors have interpreted this result in terms of a wind scenario: systems exhibiting larger equivalent widths occur in less massive, star-bursting galaxies. We note, however, several caveats to their interpretation: (i) the Mg II absorbers have $z < 1$ and may have very different characteristics (star-formation rates, metallicity, gas content) than the $z > 2$ QSO-DLAs that are plotted in Figure 6; (ii) Zibetti *et al.* (2007) find the integrated light of galaxies corresponding to Mg II absorbers is brighter for larger equivalent width systems suggesting larger masses.

Now consider the evidence in favor of interpreting the W_{1526} statistic (and perhaps Δv_{90}) as galactic-scale outflows. First, as noted above, the trend of decreasing correlation-length with increasing equivalent width offers at least qualitative evidence for a wind scenario (Bouché

⁹ In absorbers where one observes both the Si II 1526 transition and the Mg II doublet, one finds the line profiles track each other very closely. As such, their equivalent widths are highly correlated and roughly scale as the inverse of their wavelengths: $W_{1526} \approx W_{2796} \lambda_{1526} / \lambda_{2796}$ (in detail we find $W_{2796} \approx 3W_{1526}$).

et al. 2007). Second, the kinematics of some strong Mg II absorbers are consistent with that expected for symmetric outflows (Bond *et al.* 2001). Third, if star formation drives galactic-scale outflows, then one may expect a correlation between metallicity and W_{1526} . It may be difficult to precisely derive the observed trend ($[\text{M}/\text{H}] \propto 1.5 \log W_{1526}$) from first principles, but we cannot rule out such a scenario. Third, we find the Lyman break galaxy MS 1512-cB58 (Pettini *et al.* 2002) lies directly on the W_{1526} - $[\text{M}/\text{H}]$ trend of the QSO-DLAs (black diamond in Figure 6b). Given that the LBG gas kinematics are dominated by outflows (Pettini *et al.* 2002), the correspondence between the LBG data and the QSO-DLA trend is at least suggestive that outflows may play a role in shaping the observed correlation. The comparison with the QSO-DLAs may not be appropriate, however, because the LBG sightline is restricted to originate at the central, star-forming region of the galaxy. This implies a special impact parameter and one that presumably probes only half of the total velocity field. In these respects, a comparison with the GRB-DLAs is more appropriate and the correspondence with the QSO-DLA trend may be simple coincidence.

There are several arguments against interpreting the W_{1526} measurements as galactic-scale outflows. First, the similarity in the W_{1526} and Δv_{90} - $[\text{M}/\text{H}]$ trends would require one to interpret both statistics in terms of outflows (or invoke coincidence). In turn, one would have to argue that these winds have gas with large neutral fractions (Prochaska *et al.* 2002) and significant cross-section to gas with $N_{\text{HI}} > 10^{21} \text{ cm}^{-2}$ (e.g. Schaye 2001). Second, we believe a galactic-scale outflow scenario would be severely challenged to reproduce the tight correlation observed for W_{1526} and metallicity. Assuming outflows are generally collimated, the W_{1526} statistic should exhibit a wide range of values for a given wind speed as a function of the sightline configuration (i.e. impact parameter and inclination). Furthermore, the W_{1526} value is given by the internal dynamics of the wind (i.e. its turbulence) because it is a relative measure independent of the systemic velocity. It is not obvious that this quantity could be tightly correlated with metallicity. Third, there are at least some GRB-DLAs where the W_{1526} velocity field is not strictly consistent with outflows (Figure 9). Fourth, mass-metallicity relations have been identified

for numerous galaxy populations at a range of redshifts (Dekel & Woo 2003; Tremonti *et al.* 2004; Kobulnicky & Kewley 2004; Savaglio *et al.* 2005; Erb *et al.* 2006). It would be very remarkable for the QSO-DLAs to exhibit a tight velocity-metallicity trend that was unrelated to a mass-metallicity correlation. Fifth, we question a scenario which requires galactic-scale outflows in all galaxies tuned to give both low and large W_{1526} values with such small scatter. Sixth, comparisons of Mg II absorption line profiles with H II emission-line kinematics are inconsistent with a wind scenario and support dynamical motions (Steidel *et al.* 2002). Finally, while observers are quick to invoke outflows to explain extreme velocity fields, we question whether outflows can reasonably explain widths approaching and in excess of 1000 km s^{-1} .

On balance, we currently favor the interpretation of the velocity fields in QSO-DLAs as being dominated by gravitational motions, at least for $W_{1526} < 1.5 \text{ \AA}$ and $\Delta v_{90} < 200 \text{ km s}^{-1}$. At large W_{1526} and large Δv_{90} , it is reasonable to expect that additional velocity fields contribute. Indeed, an inspection of Figure 6b reveals that the QSO-DLA galaxies with largest departure from the $[\text{M}/\text{H}]$ - W_{1526} relation occur at large W_{1526} values. These few QSO-DLAs have especially large W_{1526} for their observed metallicity and/or low metallicity for the observed W_{1526} value. We suspect that the former inference is the correct interpretation and that these systems have contributions to the W_{1526} statistic beyond the halo gas dynamics. These QSO-DLAs are the most viable candidates for sightlines penetrating galactic-scale outflows. This interpretation could also explain the frequency of GRB-DLAs that lie off the QSO-DLA trend. As noted in the previous section, GRB-DLAs have especially large specific star formation rates. Therefore, GRB may flag galaxies at a time when they are most likely to drive galactic-scale outflows. Given the identification of GRB with massive, short-lived stars, there may not be sufficient time to drive these winds with supernovae feedback. Instead, one may need to consider merger-driven, galactic outflows.

We wish to thank A. Dekel, A. Maller, D. Lin, E. Ramirez-Ruiz, P. Bodenheimer, J. Hennawi, S. Ellison, S. Burles, and R. Bernstein for valuable discussions.

REFERENCES

Barth, A. J. *et al.* 2003, ApJ (Letters), 584, L47.
 Berger, E. *et al.* 2006, ApJ, 642, 979.
 Bergeron, J. and Boisse, P. 1991, Advances in Space Research, 11, 241.
 Bond, N. A. *et al.* 2001, ApJ, 562, 641.
 Bouché, N. *et al.* 2005, ApJ, 628, 89.
 Bouché, N. *et al.* 2007, New Astronomy Review, 51, 131.
 Castro, S. *et al.* 2003, ApJ, 586, 128.
 Cen, R. and Ostriker, J. P. 2000, ApJ, 538, 83.
 Charlton, J. C. and Churchill, C. W. 1998, ApJ, 499, 181.
 Chen, H.-W. and Lanzetta, K. M. 2003, ApJ, 597, 706.
 Chen, H.-W., Lanzetta, K. M., and Webb, J. K. 2001, ApJ, 556, 158.
 Chen, H.-W. *et al.* 2007, ArXiv Astrophysics e-prints.
 Chen, H.-W. *et al.* 2005, ApJ, 634, L25.
 Christensen, L., Hjorth, J., and Gorosabel, J. 2004, A&A, 425, 913.
 Colbert, J. W. and Malkan, M. A. 2002, ApJ, 566, 51.
 Cooke, J. *et al.* 2006, ApJ, 636, L9.
 Cox, T. J. *et al.* 2006, MNRAS, 373, 1013.
 Dekel, A. and Woo, J. 2003, MNRAS, 344, 1131.
 Dekker, H. *et al.* 2000, in Proc. SPIE Vol. 4008, p. 534-545, Optical and IR Telescope Instrumentation and Detectors, Masanori Iye; Alan F. Moorwood; Eds., ed. M. Iye and A. F. Moorwood, 534.
 Dessauges-Zavadsky, M. *et al.* 2006, A&A, 445, 93.
 Dong, S., Lin, D. N. C., and Murray, S. D. 2003, ApJ, 596, 930.
 Erb, D. K. *et al.* 2006, ApJ, 644, 813.
 Fiore, F. *et al.* 2005, ApJ, 624, 853.
 Fruchter, A. S. *et al.* 2006, Nature, 441, 463.
 Fynbo, J. P. U. *et al.* 2006, A&A, 451, L47.
 Haehnelt, M. G., Steinmetz, M., and Rauch, M. 1998, ApJ, 495, 647.
 Haehnelt, M. G., Steinmetz, M., and Rauch, M. 2000, ApJ, 534, 594.
 Herbert-Fort, S. *et al.* 2006, PASP, 118, 1077.
 Jedamzik, K. and Prochaska, J. X. 1998, MNRAS, 296, 430.
 Kauffmann, G. 1996, MNRAS, 281, 475.
 Kawai, N. *et al.* 2006, Nature, 440, 184.
 Kobulnicky, H. A. and Kewley, L. J. 2004, ApJ, 617, 240.
 Lanzetta, K. M. and Bowen, D. 1990, ApJ, 357, 321.
 Lanzetta, K. M. and Bowen, D. V. 1992, ApJ, 391, 48.

Le Floc'h, E. *et al.* 2003, A&A, 400, 499.

Ledoux, C. *et al.* 2006, A&A, 457, 71.

Ledoux, C., Petitjean, P., and Srianand, R. 2003, MNRAS, 346, 209.

Lee, H. *et al.* 2006, ApJ, 647, 970.

Lehner, N. and Howk, J. C. 2007, ArXiv Astrophysics e-prints.

Mac Low, M.-M. and Ferrara, A. 1999, ApJ, 513, 142.

Maller, A. *et al.* 2000, in ASP Conf. Ser. 200: Clustering at High Redshift, ed. A. Mazure, O. Le Fèvre, and V. Le Brun, 430.

Maller, A. H. *et al.* 2001, MNRAS, 326, 1475.

Maller, A. H. *et al.* 2003, MNRAS, 343, 268.

McDonald, P. and Miralda-Escudé, J. 1999, ApJ, 519, 486.

Metzger, M. R. *et al.* 1997, Nature, 387, 879.

Mirabal, N. *et al.* 2002, ApJ, 578, 818.

Mo, H. J., Mao, S., and White, S. D. M. 1998, MNRAS, 295, 319.

Mo, H. J. and Miralda-Escudé, J. 1996, ApJ, 469, 589.

Möller, P., Fynbo, J. P. U., and Fall, S. M. 2004, A&A, 422, L33.

Møller, P. *et al.* 2002, ApJ, 574, 51.

Murphy, M. T. *et al.* 2007, ArXiv Astrophysics e-prints.

Nagamine, K. *et al.* 2005, ArXiv Astrophysics e-prints.

Nulsen, P. E. J., Barcons, X., and Fabian, A. C. 1998, MNRAS, 301, 168.

Pettini, M. *et al.* 2002, ApJ, 569, 742.

Pettini, M. *et al.* 2001, ApJ, 554, 981.

Pettini, M. *et al.* 1994, ApJ, 426, 79.

Piranomonte, S. *et al.* 2007, A&A.

Prochaska, J. X. 1999, ApJ, 511, L71.

Prochaska, J. X., Chen, H.-W., and Bloom, J. S. 2006, ApJ, 648, 95.

Prochaska, J. X. *et al.* 2007a, ApJS, 168, 231.

Prochaska, J. X., Chen, H.-W., Dessauges-Zavadsky, M., and Bloom, J. S. 2007, ApJ, submitted.

Prochaska, J. X. *et al.* 2003, ApJ, 595, L9.

Prochaska, J. X. *et al.* 2002, PASP, 114, 933.

Prochaska, J. X., Herbert-Fort, S., and Wolfe, A. M. 2005, ApJ, 635, 123.

Prochaska, J. X. and Wolfe, A. M. 1997, ApJ, 487, 73.

Prochaska, J. X. and Wolfe, A. M. 1998, ApJ, 507, 113.

Prochaska, J. X. and Wolfe, A. M. 2001, ApJ, 560, L33.

Prochaska, J. X. *et al.* 2007b, ArXiv Astrophysics e-prints.

Prochter, G. *et al.* 2006, In prep.

Prochter, G. E., Prochaska, J. X., and Burles, S. M. 2006, ApJ, 639, 766.

Rao, S. M., Turnshek, D. A., and Nestor, D. B. 2006, ApJ, 636, 610.

Razoumov, A. O. *et al.* 2006, ApJ, 645, 55.

Savage, B. D., Sembach, K. R., and Lu, L. 1997, AJ, 113, 2158.

Savaglio, S., Fall, S. M., and Fiore, F. 2003, ApJ, 585, 638.

Savaglio, S. *et al.* 2005, ApJ, 635, 260.

Schaye, J. 2001, ApJ, 559, L1.

Sheinis, A. I. *et al.* 2000, in Proc. SPIE Vol. 4008, p. 522-533, Optical and IR Telescope Instrumentation and Detectors, Masanori Iye; Alan F. Moorwood; Eds., 522.

Shin, M.-S. *et al.* 2006, ArXiv Astrophysics e-prints.

Spitzer, L. J. 1990, ARA&A, 28, 71.

Steidel, C. C. 1993, in ASSL Vol. 188: The Environment and Evolution of Galaxies, ed. J. M. Shull and H. A. Thronson, 263.

Steidel, C. C. *et al.* 2002, ApJ, 570, 526.

Steidel, C. C. and Sargent, W. L. W. 1992, ApJS, 80, 1.

Tassis, K., Kravtsov, A. V., and Gnedin, N. Y. 2006, ArXiv Astrophysics e-prints.

Thoene, C. C. *et al.* 2006, ArXiv Astrophysics e-prints.

Tremonti, C. A. *et al.* 2004, ApJ, 613, 898.

Tumlinson, J. *et al.* 2007, In prep.

Vladilo, G. *et al.* 2001, ApJ, 557, 1007.

Vogt, S. S. *et al.* 1994, in Proc. SPIE Instrumentation in Astronomy VIII, David L. Crawford; Eric R. Craine; Eds., Volume 2198, p. 362, 362.

Vreeswijk, P. M. *et al.* 2004, A&A, 419, 927.

Vreeswijk, P. M. *et al.* 2006, A&A, 447, 145.

Watson, D. *et al.* 2006, ApJ, 652, 1011.

Wolfe, A. M., Gawiser, E., and Prochaska, J. X. 2005, ARA&A, 43, 861.

Wolfe, A. M. *et al.* 1995, ApJ, 454, 698.

Wolfe, A. M. and Prochaska, J. X. 1998, ApJ, 494, L15+.

Wolfe, A. M. and Prochaska, J. X. 2000a, ApJ, 545, 591.

Wolfe, A. M. and Prochaska, J. X. 2000b, ApJ, 545, 603.

Wolfe, A. M., Prochaska, J. X., and Gawiser, E. 2003, ApJ, 593, 215.

Wolfe, A. M. *et al.* 1986, ApJS, 61, 249.

Zibetti, S. *et al.* 2007, ApJ, 658, 161.

Zwaan, M. A. and Prochaska, J. X. 2006, ApJ, 643, 675.